Supporting Information

Cellulose nanocrystals of variable sulfation degree can sequester specific platelet lysate-derived biomolecules to modulate stem cells response

Bárbara B. Mendes, Manuel Gómez-Florit, Hugo Osório, Adriana Vilaça, Rui M. A. Domingues, Rui L. Reis, Manuela E. Gomes

Experimental section

1. Precursors preparation

Preparation of platelet lysate (PL): Platelet concentrate collections, obtained from volunteer donation from healthy donors as by 2005/62/CE, were performed at *Serviço de Imuno-Hemoterapia – Centro Hospitalar de São João* (Portugal) provided under an approved institutional board protocol (ethical commission of CHSJ/FMUP approved at 18/13/2018). Platelet batches are obtained from a pool of donors of platelet concentrates from whole blood differential centrifugations or platelet apheresis.[1-4] Then, PL was prepared in-house from a pool of twelve platelet concentrates that were subjected to three temperature cycles (-196 °C and 37 °C), and stored at -80 °C. Just before use, PL was thawed at RT, centrifuged at 4000 x g for 5 minutes and filtered through a 0.45 μm pore filter to remove any cell debris or clots.

Preparation of cellulose nanocrystals (CNC): CNC were extracted from microcrystalline cellulose (MCC) powder (Sigma-Aldrich, USA) by sulfuric acid hydrolysis according to Bondeson with minor modifications.[5] In brief, 42 g of MCC was mixed with 189 mL of deionized water (DI). DI/MCC suspension was then put in an ice bath and stirred using a mechanical agitator (500 rpm) for 10 minutes. 188.3 mL of concentrated sulfuric acid (95−98% from Sigma-Aldrich, USA) was added dropwise up to a final concentration of 64 wt.%. The suspension was heated to 44 °C while stirring at 500 rpm for 120 min. The reaction was stopped by diluting the suspension with cold water

(5x) and left to decant at 4 °C. The supernatant was discarded, and the remaining suspension was centrifuged for 10 minutes at 9000 rpm and 5 °C. The supernatant was successively replaced with DI water and the suspension subjected to centrifugation cycles until the supernatant became turbid. The resulting suspension was collected and extensively dialyzed using cellulose dialysis membrane MWCO: 12-14 kDa (Sigma-Aldrich, USA) against DI water until neutral pH. After dialysis the content was sonicated three times (VCX-130PB-220, Sonics) for 10 minutes using an ultrasound probe at 60% of amplitude output, under ice cooling to prevent overheating. The cloudy suspension was centrifuged one last time to remove big particulates and the final supernatant containing the CNC (high -SO_3H content, High) was stored at 4 °C until further use.

Preparation of CNC of variable surface sulfation degrees: Custom-made stainless steel autoclaves of height 12 cm and diameter 6 cm (Neves & Neves Metalomecânica, Portugal) were used during hydrothermal treatment of aqueous CNC suspensions. Briefly, an aqueous suspension of CNC (90 mL, 1 wt. %) was added to a glass flask, while the autoclave was sealed and heated to 120 °C for 30 min. Then, the glass flask was placed inside the autoclave for 3 h (medium -SO_3H content, Medium) or 6 h (low -SO_3H content, Low) at 120 °C in a self-pressurizing environment. After cooling the autoclave to RT for 1 hour, the resulting CNC suspension was collected and extensively dialyzed using cellulose dialysis membrane MWCO: 12-14 kDa (Sigma-Aldrich, USA) against DI water until neutral pH to remove the sulfuric acid product from CNC solution. The final suspension was stored at 4 ºC until further characterization was performed.

Preparation of aldehyde-functionalized CNC (a-CNC): Vicinal hydroxyl groups on CNC's surface were converted to carbonyls by adding sodium periodate ($NaIO_4$) in a 1:1 molar ratio for 12 hours.[6] In a typical experiment, $NaIO_4$ (Sigma-Aldrich, USA) was added to CNC aqueous suspension (1 wt.%) in a 1:1 molar ratio ($NaIO_4$:CNC). The

mixture was allowed to stir at RT for 12 hours preventing from light exposure. Unreacted periodate was quenched by the addition of excess of ethylene glycol (Sigma-Aldrich, USA). The mixture was transferred into a dialysis membrane (cellulose dialysis membrane MWCO: 12-14 kDa) and dialyzed against DI water for 3 days with regular water replacement. The final working suspension of modified CNC was collected and stored at 4 °C.

2. Precursors characterization

Morphological characterization of CNC: CNC morphology was analyzed by Atomic Force Microscopy (AFM). One drop of each diluted solution of 0.0015 wt. % CNC in DI water was dropped on freshly cleaved mica discs (9.9 mm diam. and 0.27 thick). The suspension was left to adsorb for 15 min and the excess liquid was removed. The disc was washed two times with ultrapure water (Milli-Q, 18.2 M $\Omega.cm^{-1}$) to remove particles excess and allowed to dry overnight at RT. The samples were imaged in tapping mode with a MultiMode atomic force microscopy (AFM, Bruker, USA). The obtained images were treated and analyzed using Gwyddion software (version 2.53) to measure the length and height of CNC formulations. At least 50 particles were randomly selected from different AFM images.

Quantification of CNC sulfation degree: The CNC sulfate content was determined following the ion-exchange resin treatment and conductometric titration of CNC according to Beck, S. et al.[7] Dowex marathon C hydrogen from strong acid action exchange resin (Sigma-Aldrich, USA) that fully protonates CNC sulfate half-ester groups was immersed in ultrapure water for 30 min and poured into glass Econo-Column® chromatography columns (2.5 × 30 cm, Bio-Rad Laboratories, USA) with a porous polymer bed support at the bottom. CNC suspensions (100 mL, 0.5 wt.%) was fed from the top of the column at 3-4 $mL.min^{-1}$, and the initial 1-2 bed volumes were

discarded to avoid excessive sample dilution. The resin-to-CNC mass ratios was approximately 20.8 (0.5 g of CNC to 10.4 g of resin). Then, sulfate half-ester content was determined via conductometric titration. Briefly, 113 mg of resin-treated CNC and 0.0117g (1 mM NaCl aqueous solution) were dispersed in a final volume of 200 mL of ultrapure water. Samples were treated with 10 mM NaOH (Sigma-Aldrich, USA) added in 0.1 mL increments. Titration conductivity values were corrected for dilution effects and sulfate half-ester groups content (mmol.kg^{-1} CNC) was calculated using Equation S1.

$$R - OSO_3H = \frac{V_{NaOH} C_{NaOH}}{m_{CNC}} \quad \text{(Equation S1)}$$

Where V_{NaOH} (mL) is the inset equivalence point determined from conductometric titration curve, C_{NaOH} (mol.L^{-1}) is the concentration of titration used and m_{cnc} (g) is the mass of the CNC suspension.

Surface charge: Zeta potential of the different a-CNC formulations at concentration of 1 mg. mL^{-1} in water was determined (n=3) using a zetasizer (Nano ZS, Malvern Instruments).

3. Protein corona characterization

Incubation of CNC with PL-derived proteins: Prior to corona preparation, a-CNC solutions (High, Medium and Low) were diluted with ultrapure water to a final concentration of 2 mg. mL^{-1}. Afterwards, 1900 µL of CNC dispersions (containing 3.8 mg of CNC) were incubated with 1900 µL PL solution (containing 128.44 mg of total protein content) for 90 min at 37 °C under constant agitation (200 rpm) for a final CNC concentration of 1 mg. mL^{-1}. CNC were separated from the supernatant by centrifugation at 15000 × g for 30 min. The particle pellet was resuspended in phosphate-buffered saline (PBS) and washed by three centrifugation steps at 15000 × g for 30 min, and subsequently

re-dispersed in 60 µL of ultrapure water and freezed until further analysis. The proteins adsorbed on CNC surface after the first centrifugation are called as 'soft' corona, whereas CNC-PL complexes that were successively washed to remove the unbound or loosely bound proteins ('soft' corona) are called as 'hard' corona.

Sodium dodecyl sulphate polyacrylic gel electrophoresis (SDS-PAGE): 20 µl of non-reducing sodium dodecyl sulphate (SDS) sample buffer, which was prepared using 4% w/v SDS, 20% v/v glycerol, 10% w/v 2-mercaptoethanol, 0.05% w/v bromophenol blue, 125 mM TRIS-HCl to pH 6.8, was added to the 'soft' and 'hard' corona PL-CNC complexes. Pellet was dispersed by vortexing and heating for 5 min at 95 ˚C. PL-protein complexes were thus shattered, and CNC were removed by centrifugation at 12300 × g for 15 min. Aliquots of adsorbed proteins (10 µL) were loaded on SDS-polyacrylamide gel using 3% v/v stacking and 12.5% v/v separation polyacrylamide gels prepared according to manufacturer's protocol (SDS Gel Preparation kit, Sigma Aldrich, USA) in SDS running buffer (0.1 % w/v SDS, 25 mM TRIS base, 192 mM glycine). Electrophoresis was carried out at 75 V for 15 min and then at 150 V for 1 h (BioRad, USA). After electrophoresis, the gels were stained with Coomassie Brilliant blue staining (1 g Commassie Brillant Blue, 500 mL methanol, 100 mL glacial acetic acid in 1 L of DI water) for 1 h, de-stain I solution (80 mL methanol, 20 mL acetic acid in 200 mL of DI water) for 45 min and then de-stain II solution (12.5 mL methanol, 17.5 mL acetic acid in 220 mL of DI water) for 45 min. The molecular weight of PL-CNC proteins complexes was calculated by analyzing their area using FIJI software gel analysis tools.[8]

Mass spectrometry: Proteins were solubilized with 100 mM Tris pH 8.5, 1% sodium deoxycholate, 10 mM tris(2-carboxyethyl)phosphine (TCEP), 40 mM chloroacetamide and protease inhibitors for 10 minutes at 95ºC at 1000 rpm (Thermomixer, Eppendorf). Each sample was processed for proteomics analysis following the solid-phase-enhanced

sample-preparation (SP3) protocol as described in PMID30464214. Enzymatic digestion was performed with Trypsin/LysC (2 micrograms) overnight at 37ºC at 1000 rpm.

Protein identification and quantitation was performed by nanoLC-MS/MS. This equipment is composed by an Ultimate 3000 liquid chromatography system coupled to a Q-Exactive Hybrid Quadrupole-Orbitrap mass spectrometer (Thermo Scientific, Bremen, Germany). Samples were loaded onto a trapping cartridge (Acclaim PepMap C18 100Å, 5 mm x 300 µm i.d., 160454, Thermo Scientific) in a mobile phase of 2% ACN, 0.1% FA at 10 µL/min. After 3 min loading, the trap column was switched in-line to a 50 cm by 75µm inner diameter EASY-Spray column (ES803, PepMap RSLC, C18, 2 µm, Thermo Scientific, Bremen, Germany) at 250 nL/min. Separation was generated by mixing A: 0.1% FA, and B: 80% ACN, with the following gradient: 5 min (2.5% B to 10% B), 120 min (10% B to 30% B), 20 min (30% B to 50% B), 5 min (50% B to 99% B) and 10 min (hold 99% B). Subsequently, the column was equilibrated with 2.5% B for 17 min. Data acquisition was controlled by Xcalibur 4.0 and Tune 2.9 software (Thermo Scientific, Bremen, Germany).

The mass spectrometer was operated in data-dependent (dd) positive acquisition mode alternating between a full scan (*m/z* 380-1580) and subsequent HCD MS/MS of the 10 most intense peaks from full scan (normalized collision energy of 27%). ESI spray voltage was 1.9 kV. Global settings: use lock masses best (*m/z* 445.12003), lock mass injection Full MS, chrom. peak width (FWHM) 15s. Full scan settings: 70k resolution (*m/z* 200), AGC target 3e6, maximum injection time 120 ms. dd settings: minimum AGC target 8e3, intensity threshold 7.3e4, charge exclusion: unassigned, 1, 8, >8, peptide match preferred, exclude isotopes on, dynamic exclusion 45s. MS2 settings: microscans 1, resolution 35k (*m/z* 200), AGC target 2e5, maximum injection time 110 ms, isolation window 2.0 *m/z*, isolation offset 0.0 m/z, spectrum data type profile.

The raw data was processed using Proteome Discoverer 2.4.0.305 software (Thermo Scientific) and searched against the UniProt database for the *Homo sapiens* Proteome 2019_09 and NIST Human Orbitrap HCD Spectral Library. The Sequest HT search engine was used to identify tryptic peptides. The ion mass tolerance was 10 ppm for precursor ions and 0.02 Da for fragment ions. Maximum allowed missing cleavage sites was set 2. Cysteine carbamidomethylation was defined as constant modification. Methionine oxidation and protein N-terminus acetylation were defined as variable modifications. Peptide confidence was set to high. The processing node Percolator was enabled with the following settings: maximum delta Cn 0.05; decoy database search target FDR 1%, validation based on q-value. Protein label free quantitation was performed with the Minora feature detector node at the processing step. Precursor ions quantification was performing at the processing step with the following parameters: unique plus razor peptides were considered, precursor abundance was based on intensity, normalization mode was based on total peptide amount, pairwise protein ratio calculation, hypothesis test was based on t-test (background based).

UniProt entries were converted to gene name using the UniProt tool (https://www.uniprot.org/uploadlists/). The common or exclusively identified proteins were analyzed using the Venny tool (https://bioinfogp.cnb.csic.es/tools/venny/, version 2.1.0). Proteins have been grouped with regard to the biological process involved using the categories of the Panther Biological process (http://www.pantherdb.org/, version 15.0). The relative abundance of the 30 main components and selected signaling molecules were classified as Panther protein class and heat maps were done using the GraphPad PRISM v 7.0. Average presence was set to 100 (white) and red color denotes counts higher and blue denotes lower than groups average. Finally, the isoelectric point

(*pI*) of the 30 main components of CNC formulations was estimated using Isoelectric Point Calculator.[9]

4. *In vitro* cell behavior

CNC film coating preparation: Circular glass coverslips of 13 mm diameter and 1 mm thickness (Agar Scientific, UK) were first cleaned in 5:1:1 solution of H_2O:NH_3:H_2O_2 at 75 °C for 5 minutes, washed with ultrapure water, dried gently with nitrogen and finally UV/ozone treated (Vilber-lourmat, France) for 10 min. Then, 200 µL of polyethyleneimine (PEI, Sigma-Aldrich, USA, high molecular weight and branched, 20 mM in 0.5 M KCl) was spin coated (Laurell technologies, USA) for 30 s at 2000 rpm to confer a positive charge, and subsequently washed two times with ultrapure water at 500 rpm for 10 s. Afterwards, the samples were dried gently under a steady nitrogen stream, followed by adsorption of the CNC suspensions (200 µL, 1 wt. %) at stationary state for 10 s, and then at 2000 rpm for 30 s. The so-coated CNC samples were dried overnight at 60 ºC, washed two times with ultrapure water to desorb loosely bound species. AFM images were obtained using a Solver Pro-M Scanning Probe Microscope (NT-MDT) with rectangular silicon cantilever at RT (23 °C), in tapping mode (6 µm. s^{-1}). The data analysis was performed using the freeware Gwyddion 2.26. For cells experiment, the coverslips samples were rinsed with ethanol and dried in a laminar flow with sterile air.

Incubation with relevant bioactive molecules: The CNC coated coverslips were incubated with PL for 1 hour at 37 °C under constant agitation (200 rpm), and subsequently washed three times with sterile PBS.

Cell isolation and expansion: Human adipose-derived stem cells (hASCs) were obtained from lipoaspirate samples of the abdominal region of patients undergoing plastic surgery under the scope of an established protocol with Hospital da Prelada (Porto,

Portugal), and with the approval of the Hospital and University of Minho Ethics Committee. The hASCs isolation was performed using a previous optimized protocol.[10] hASCs were maintained in α-MEM supplemented with 10% FBS and 1% antibiotic/antimycotic solution at 37 ºC, 5% CO_2. hASCs were seeded onto coverslip surfaces at a density of 4000 cells per 1 cm^2. The first 2 h (initial cell adhesion) were in the culture media without serum, and then all cell culture assays of hASCs seeded onto coverslip surfaces were performed using α-MEM supplemented with 1% FBS and 1% antibiotic/antimycotic solution.

Immunofluorescence: After 2, 7 or 28 days of culture, the coverslips were washed with PBS and then fixed in 10% formalin (Thermo Fisher Scientific, USA) for 15 min at RT and permeabilized using 0.2% v/v Triton-X 100 (Sigma-Aldrich, USA). After washing, samples were blocked using 3% w/v BSA and incubated with 1:50 v/v solution of specific aggrecan primary antibody (MA316888, Thermo Fisher Scientific, USA) or 1:100 v/v solution of specific collagen type II primary antibody (MAB1330, Millipore, USA). Then, samples were incubated with 1:200 v/v Alexa Fluor® 488 conjugated secondary antibody (Thermo Fisher Scientific, USA). After washing, samples were incubated with 1:200 v/v rhodamine-conjugated phalloidin (Sigma-Aldrich, USA) for 10 min and 1:1000 v/v 4′, 6-diamidino-2-phenylindole (DAPI, Sigma-Aldrich, USA) for 20 min (dilutions in PBS). After washing, the samples were mounted in an fluoromount aqueous mounting medium (Sigma-Aldrich, USA) and observed under a confocal microscope TCS SP8 (Leica Microsystems, Germany). The expression levels of aggrecan was assessed by calculating the mean fluorescence intensity of obtained confocal images ($n > 5$) using Fiji software. Briefly, images were thresholded to separate the signal from the background, and the mean fluorescence values were calculated and

normalized by the number of nucleus (per cell). Cell proliferation was evaluated measuring cell nuclei per area using Image J software.

Staining procedures: After 28 days of culture, PL-CNC coated coverslips were washed with PBS and then fixed in 10% formalin (Thermo Fisher Scientific, USA) for 30 min at RT. The samples were stained with alcian blue (1% w/v alcian blue solution in 3% v/v acetic acid) for h. For alizarin red staining (2% v/v alizarin solution at pH 4.1-4.3), the samples were immersed for 5 min. Finally, the samples were also stained with oil red O staining (0.5% v/v oil red in isopropanol, and then dilute 3 mL of the stock solution in 2 mL of water) for 25 min. All formulations were washed three times with PBS and then mounted in an fluoromount aqueous mounting medium (Sigma-Aldrich, USA). The transmitted light microscope (Zeiss, Germany) was used to observe the stained formulations. The Alcian Blue coverage area was calculated using Fiji software ($n > 10$). Briefly, images were thresholded to separate the signal from the background, and the area fraction was determined.

Statistical analysis: The statistical analysis of data was performed using GraphPad PRISM v 7.0. Shapiro-Wilk normality test and one-way or two-way analysis of variance (ANOVA) was used to analyze experimental data, followed by Tukey posthoc test for multiple comparisons. Statistical significance was set to *, $P < 0.05$; **, $P < 0.01$; $^{\alpha\alpha\alpha}$, $P < 0.001$; **** and $^{\alpha\alpha\alpha\alpha}$, $P < 0.0001$. Results are presented as mean ± standard deviation.

Supplemental results and discussion

Morphological and chemical characterization of modified CNC.

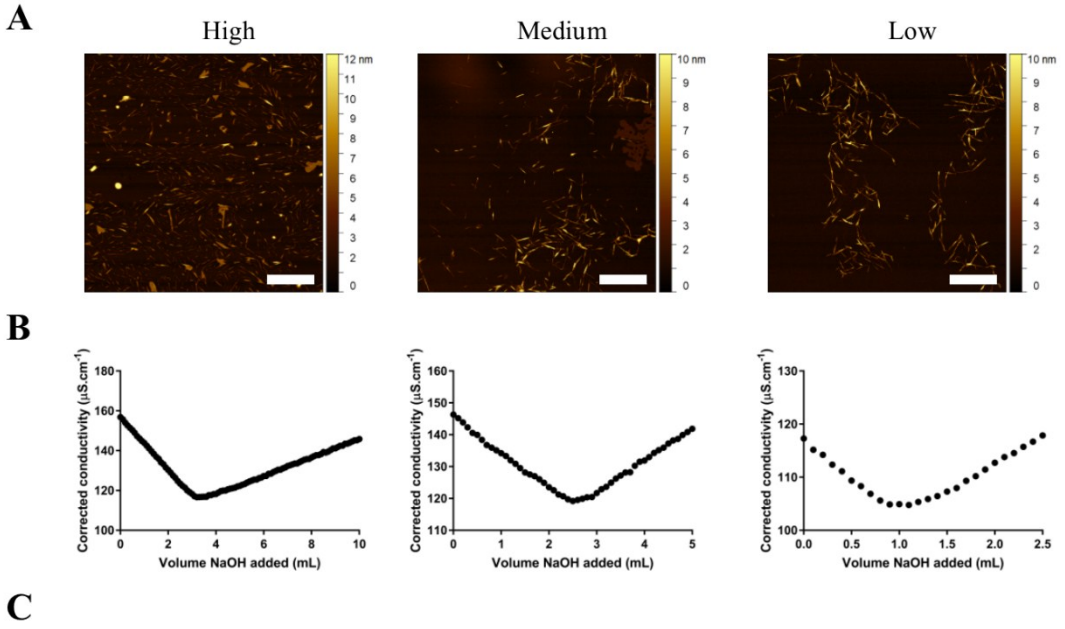

C

High	Medium	Low
- 43.9 ± 3.44 mV	- 27.7 ± 2.17 mV	- 16.2 ± 1.10 mV

Figure S1. Morphological and chemical characterization of CNC with different sulfation degrees (High, Medium and Low). (A) AFM images of modified CNC at 5x5 µm. (B) Conductometric titration curve of modified CNC to calculate sulfation degree. (C) Surface charge of the different a-CNC formulations. Scale bar: 1 µm (A).

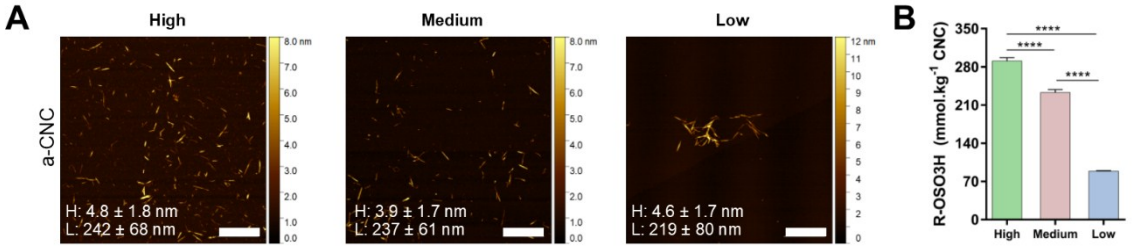

Figure S2. Morphological and chemical characterization of CNC. (A) AFM images of aldehyde-modified CNCs. (C) Sulfate group quantification determined by conductometric titration. Scale bar: 1 mm (A). H: height and L: length.

Protein corona characterization.

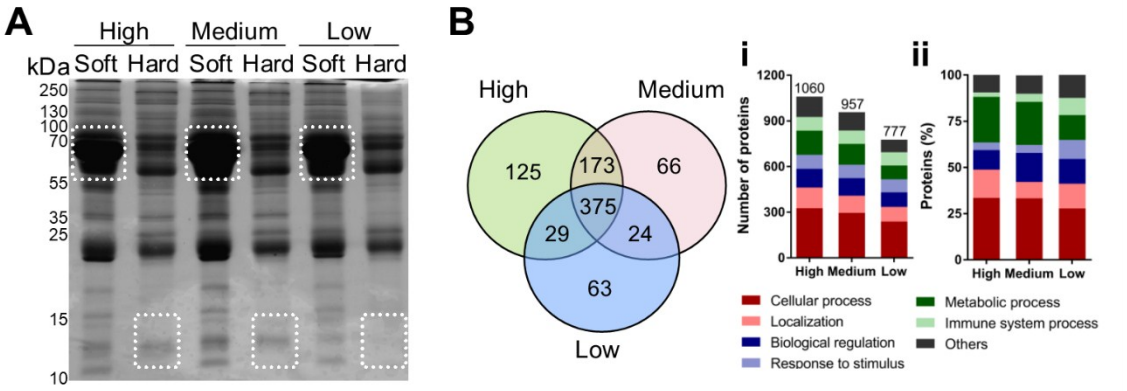

Fig. S3. (A) Protein profile in SDS-PAGE gel. (B) Analysis of 'hard' corona; venn diagram of identified proteins. Proteins were classified by their biological process and displayed as (i) number of proteins considering all identified proteins and (ii) protein (%) considering only the exclusive proteins of each group.

The 30 most abundant proteins identified in CNC coronas (Table S1) were grouped in negatively charged (pI<7), neutral (7<pI<8) and positively charged (pI>8) proteins, Table S2.

The sum of protein abundances for each group is shown in Fig. S2. H-CNC hard corona is richer in negatively charged proteins than M-CNC and L-CNC. Negatively charged proteins derived from human serum (main components of PL) such as complement protein C3 (pI=5.77), fibrinogen alpha chain (pI=5.49) or serum albumin (pI=5.57) are among the most abundant in the hard corona of H-CNC. On the other hand, all CNC formulations show considerably (one to two orders of magnitude) lower contents of positively charged than of negatively charged or neutral proteins in the hard corona. Moreover, similar contents of positively charged proteins are observed in the different CNC formulations, irrespective of their sulfation degrees.

Remarkably, these patterns of corona composition diverge from what would be expected in a system were electrostatic forces dominate the protein-nanoparticle

interactions. Although they certainly have a relevant contribution for the development of CNC hard coronas, these results suggest that electrostatic interactions are not the main driving mechanism of this process, supporting the hypothesis that nanoparticle surface chemistry might have a more determinate role on their composition.

Table S1. Main components found in high, medium and low sulfated 'hard' corona formulations by mass spectrometry analysis, listed according to their relative abundance.

N	High	Medium	Low
1	Apolipoprotein B-100	Immunoglobulin heavy constant gamma 1	Serum albumin
2	Immunoglobulin heavy constant gamma 1	Complement C3	Immunoglobulin heavy constant gamma 1
3	Complement C3	Apolipoprotein B-100	Complement C3
4	Immunoglobulin kappa constant	Serum albumin	Immunoglobulin kappa constant
5	Fibrinogen alpha chain	Immunoglobulin kappa constant	Immunoglobulin heavy constant um
6	Complement C4-A	Complement C4-A	Fibrinogen alpha chain
7	Immunoglobulin heavy constant mu	Immunoglobulin heavy constant mu	Immunoglobulin heavy constant gamma 2
8	Serum albumin	Fibrinogen alpha chain	Fibrinogen beta chain
9	Apolipoprotein E	Immunoglobulin heavy constant gamma 3	Complement C4-A
10	Myosin-9	Talin-1	Fibrinogen gamma chain
11	Talin-1	Apolipoprotein E	Immunoglobulin heavy constant alpha 1
12	Filamin-A	Filamin-A	Immunoglobulin lambda-like polypeptide 5
13	Fibronectin	Immunoglobulin lambda constant 3	Filamin-A

14	Immunoglobulin heavy constant gamma 3	Myosin-9	Complement C1q subcomponent subunit C
15	cDNA FLJ55673, highly similar to Complement factor B	Clusterin	Serotransferrin
16	Immunoglobulin lambda-like polypeptide 5	Complement C1s subcomponent	Talin-1
17	Complement factor H	Fibrinogen beta chain	Complement C1s subcomponent
18	Fibrinogen beta chain	Immunoglobulin heavy constant alpha 1	Apolipoprotein A-I
19	Clusterin	cDNA FLJ55673, highly similar to Complement factor B	Myosin-9
20	Fibrinogen gamma chain	Complement factor H	Complement C1q subcomponent subunit B
21	Complement C1q subcomponent subunit C	Complement C1q subcomponent subunit C	Apolipoprotein B-100
22	Immunoglobulin heavy constant alpha 1	Thrombospondin-1	Immunoglobulin kappa variable 3-20
23	Complement C1s subcomponent 1	Plasma kallikrein	Complement C1q subcomponent subunit A
24	Apolipoprotein A-I	Fibrinogen gamma chain	Immunoglobulin lambda constant 3
25	Thrombospondin-1	Immunoglobulin lambda variable 1-44	Alpha-1-antitrypsin
26	Platelet factor 4	Complement C1q subcomponent subunit A	Complement C1r subcomponent
27	Complement C1q subcomponent subunit B	Platelet basic protein	Complement factor H
28	Plasma kallikrein	Platelet factor 4	Immunoglobulin kappa variable 2-28
29	Histidine-rich glycoprotein	Phosphoglycerate kinase 1	Haptoglobin
30	Pigment epithelium-derived factor	Fibronectin	Alpha-2-macroglobulin

Table S2. Collective list of the thirty most abundant proteins detected in the hard coronas of each of the CNC with different sulfation degree and their respective molecular weight (Mw), isoelectric point (*pI*) and relative abundance values obtained by mass spectrometry. Proteins are sorted by ascending *pI*. (AU – arbitrary units).

UNIPROT Accession	Description	Mw (kDa)	*pI*	Protein abundance (mean values, AU)		
				High	Medium	Low
TSP1_HUMAN	Thrombospondin-1	129,3	4,51	1,49E+09	1,14E+09	9,38E+07
C1S_HUMAN	Complement C1s subcomponent	76,6	4,76	1,60E+09	1,42E+09	9,09E+08
KV320_HUMAN	Immunoglobulin kappa variable 3-20	12,5	4,77	1,85E+08	1,08E+08	5,67E+08
LV144_HUMAN	Immunoglobulin lambda variable 1-44	12,2	4,8	2,96E+08	9,55E+08	1,65E+08
A1AT_HUMAN	Alpha-1-antitrypsin	46,7	5,11	4,54E+08	2,70E+08	4,38E+08
FINC_HUMAN	Fibronectin	272,2	5,16	3,67E+09	8,18E+08	1,22E+08
FIBG_HUMAN	Fibrinogen gamma chain	51,5	5,2	2,00E+09	1,10E+09	1,88E+09
MYH9_HUMAN	Myosin-9	226,4	5,39	5,48E+09	1,49E+09	7,68E+08
APOA1_HUMAN	Apolipoprotein A-I	30,8	5,41	1,57E+09	7,32E+08	8,47E+08
KV228_HUMAN	Immunoglobulin kappa variable 2-28	12,9	5,43	2,25E+08	1,56E+08	3,53E+08
FLNA_HUMAN	Filamin-A	280,6	5,48	3,76E+09	2,29E+09	1,43E+09
FIBA_HUMAN	Fibrinogen alpha chain	94,9	5,49	9,23E+09	3,42E+09	4,22E+09
APOE_HUMAN	Apolipoprotein E	36,1	5,55	5,73E+09	2,36E+09	1,80E+08
C1R_HUMAN	Complement C1r subcomponent	81,8	5,57	4,72E+08	3,28E+08	3,81E+08
TLN1_HUMAN	Talin-1	269,6	5,58	4,98E+09	2,90E+09	1,01E+09
CLUS_HUMAN	Clusterin	52,5	5,65	2,45E+09	1,48E+09	1,05E+08
ALBU_HUMAN	Serum albumin	69,3	5,67	6,09E+09	5,90E+09	1,95E+10
PEDF_HUMAN	Pigment epithelium-derived factor	46,3	5,73	9,45E+08	5,73E+08	7,51E+07

A2MG_HUMAN	Alpha-2-macroglobulin	163,2	5,76	2,22E+08	5,33E+07	3,13E+08
CO3_HUMAN	Complement C3	187	5,77	1,20E+10	7,54E+09	6,40E+09
IGHA1_HUMAN	Immunoglobulin heavy constant alpha 1	37,6	5,77	1,91E+09	1,37E+09	1,56E+09
HPT_HUMAN	Haptoglobin	45,2	5,83	4,09E+08	2,49E+08	3,38E+08
IGKC_HUMAN	Immunoglobulin kappa constant	11,8	5,85	9,46E+09	5,46E+09	6,26E+09
CFAH_HUMAN	Complement factor H	139	5,88	2,91E+09	1,20E+09	3,55E+08
IGHM_HUMAN	Immunoglobulin heavy constant mu	49,4	6,02	6,89E+09	4,86E+09	4,52E+09
APOB_HUMAN	Apolipoprotein B-100	515,3	6,27	1,42E+10	6,08E+09	6,42E+08
CO4A_HUMAN	Complement C4-A	192,7	6,29	7,52E+09	5,24E+09	1,95E+09
B4E1Z4	cDNA FLJ55673, highly similar to Complement factor B	140,9	6,35	3,23E+09	1,30E+09	2,14E+08
TF_HUMAN	Serotransferrin	77	6,41	3,75E+08	3,12E+08	1,17E+09
IGLC3_HUMAN	Immunoglobulin lambda constant 3	11,3	6,53	6,58E+08	2,13E+09	4,53E+08
HRG_HUMAN	Histidine-rich glycoprotein	59,5	6,66	1,04E+09	6,80E+08	1,78E+08
IGHG2_HUMAN	Immunoglobulin heavy constant gamma 2	35,9	6,76	6,99E+08	7,87E+08	3,83E+09
A0A4W9A917	Immunoglobulin heavy constant gamma 3	41,3	7,03	3,37E+09	3,37E+09	3,70E+07
PGK1_HUMAN	Phosphoglycerate kinase 1	44,6	7,28	3,39E+05	8,46E+08	4,71E+06
KLKB1_HUMAN	Plasma kallikrein	71,3	7,32	1,16E+09	1,14E+09	1,04E+08
IGHG1_HUMAN	Immunoglobulin heavy constant gamma 1	36,1	7,38	1,28E+10	1,12E+10	1,18E+10
FIBB_HUMAN	Fibrinogen beta chain	55,9	7,45	2,65E+09	1,39E+09	2,07E+09
C1QC_HUMAN	Complement C1q subcomponent subunit C	25,8	7,75	1,92E+09	1,15E+09	1,38E+09
PLF4_HUMAN	Platelet factor 4	10,8	7,89	1,19E+09	8,48E+08	7,23E+07
C1QB_HUMAN	Complement C1q subcomponent subunit B	26,7	7,95	1,16E+09	5,17E+08	7,25E+08
CXCL7_HUMAN	Platelet basic protein	13,9	8,04	8,59E+08	8,76E+08	1,31E+08
IGLL5_HUMAN	Immunoglobulin lambda-like polypeptide 5	23,1	8,13	3,03E+09	6,18E+08	1,52E+09

C1QA_HUMAN	Complement C1q subcomponent subunit A	26	8,44	6,25E+08	9,43E+08	4,91E+08

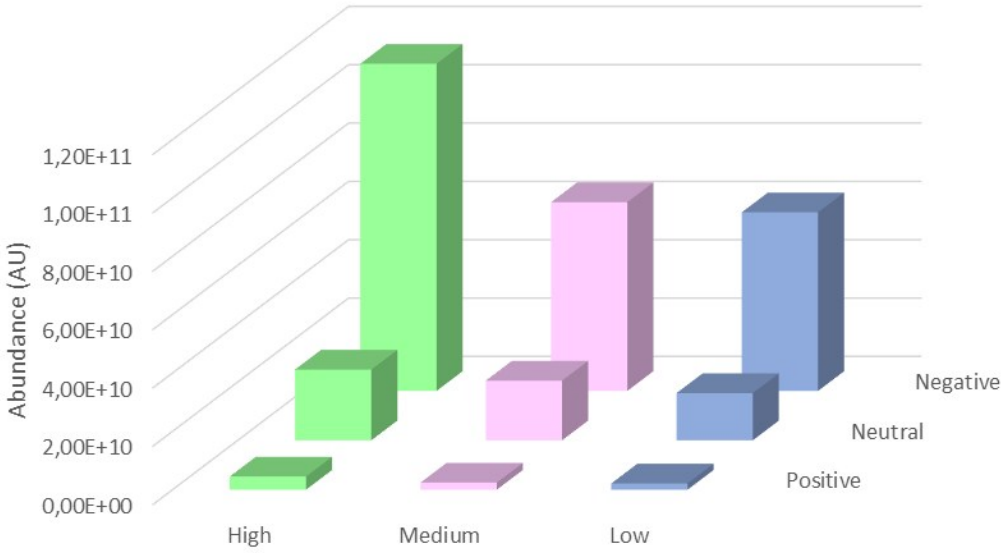

Figure S4. Sum of negatively charged (*pI*<7), neutral (7<*pI*<8) and positively charged (*pI*>8) proteins in high, medium and low sulfated 'hard' corona formulations (AU – arbitrary units).

A

Pathway description	N° protein IDs	FDR	UNIPROT IDs of matching proteins in the network
AGE-RAGE signaling pathway in diabetic complications	6	0,0124	MAPK1,MMP2,PLCB2,PRKCD,STAT5B,VEGFC
Endocytosis	8	0,0244	AP2A1,CAPZB,CHMP1B,CLTA,PDCD6IP,SH3GL1,SNX6,WAS
Necroptosis	6	0,0443	CHMP1B,EIF2AK2,H2AFV,HIST1H2AC,HIST2H2AC,STAT5B
Synaptic vesicle cycle	4	0,0443	AP2A1,ATP6V1B2,ATP6V1E1,CLTA

B

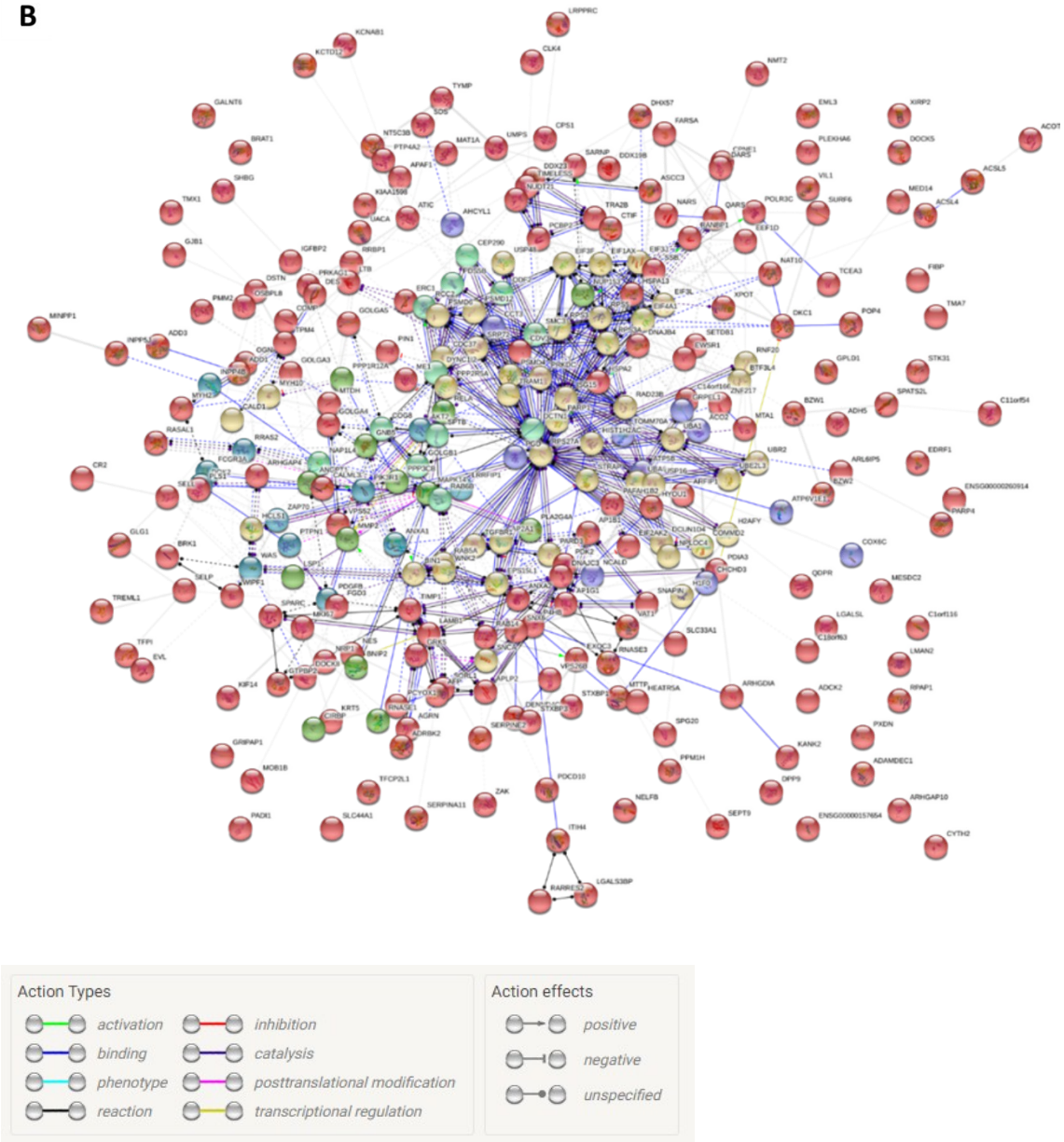

Figure S5. Enrichment in KEGG pathways (A) and networks (B) based on STRING annotation tool applied on the list of exclusively H-CNC proteins. Network edges are based on molecular action (Kmeans clustering n=6). FDR= False Discovery Rate.

A

Pathway description	N° protein IDs	FDR	UNIPROT IDs of matching proteins in the network
Non-small cell lung cancer	7	0,0045	EML4,ERBB2,MAPK3,PIK3R2,PLCG2,PRKCA,STAT5A
ErbB signaling pathway	7	0,0088	ABL1,ERBB2,MAPK3,PIK3R2,PLCG2,PRKCA,STAT5A
Ribosome	8	0,0141	RPL8,RPLP0,RPLP2,RPS15,RPS15A,RPS20,RPS3A,RPS8
Fc epsilon RI signaling pathway	6	0,0141	BTK,MAP2K3,MAPK3,PIK3R2,PLCG2,PRKCA
EGFR tyrosine kinase inhibitor resistance	6	0,0183	ERBB2,MAPK3,PDGFD,PIK3R2,PLCG2,PRKCA
Gap junction	6	0,0262	GNAQ,GUCY1A3,MAPK3,PDGFD,PRKCA,TUBA1B
VEGF signaling pathway	5	0,0264	MAPK3,MAPKAPK3,PIK3R2,PLCG2,PRKCA
HIF-1 signaling pathway	6	0,0352	ANGPT1,ERBB2,MAPK3,PIK3R2,PLCG2,PRKCA
Choline metabolism in cancer	6	0,0352	DGKA,LYPLA1,MAPK3,PDGFD,PIK3R2,PRKCA
Ras signaling pathway	9	0,0383	ABL1,ANGPT1,GNB1,MAPK3,PDGFD,PIK3R2,PLCG2,PRKCA,RALB5C
Adherens junction	5	0,0383	CSNK2A2,CSNK2B,ERBB2,LMO7,MAPK3

B

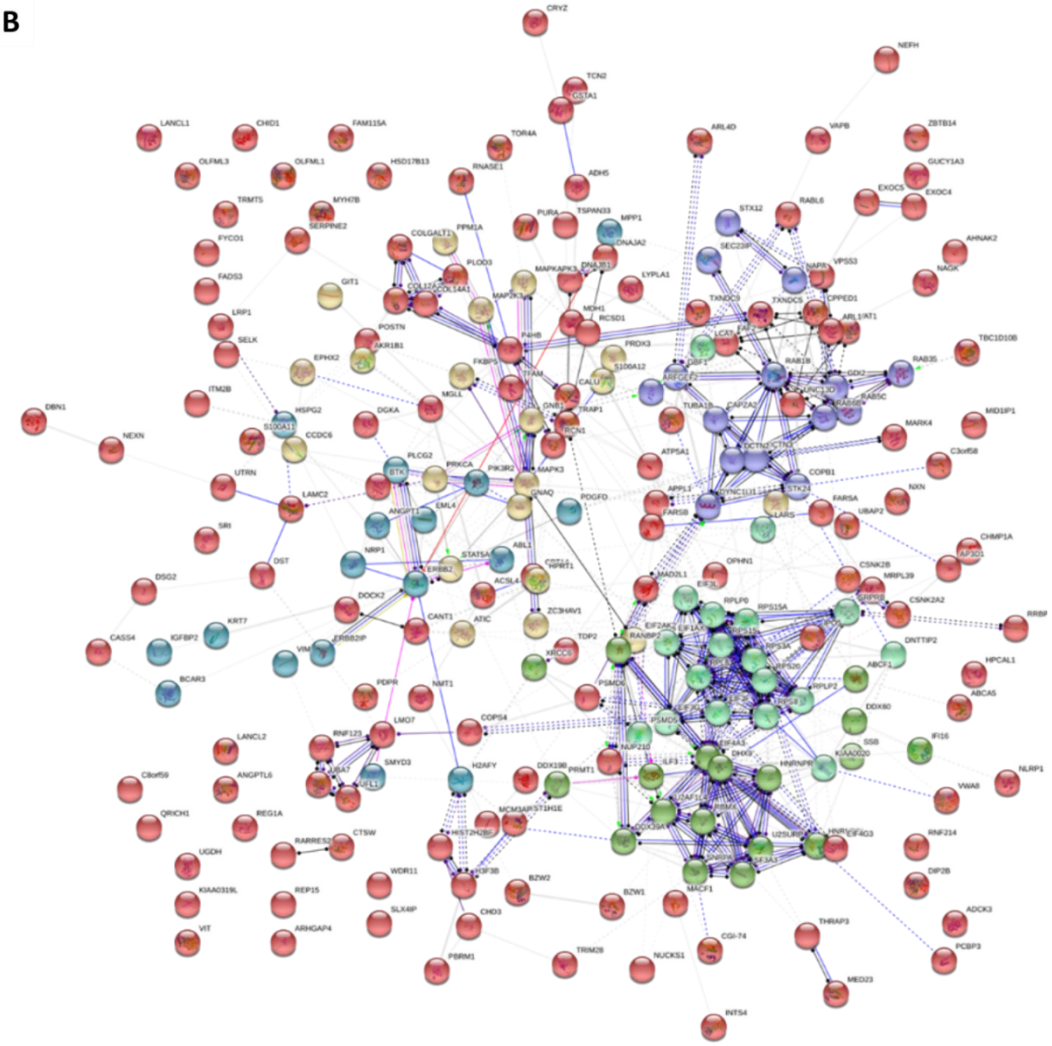

Figure S6. Enrichment in KEGG pathways (A) and networks (B) based on STRING annotation tool applied on the list of exclusively M-CNC proteins. Network edges are based on molecular action (Kmeans clustering n=6). FDR= False Discovery Rate.

A

Pathway description	Nº protein IDs	FDR	UNIPROT IDs of matching proteins in the network
Proteasome	6	0,0023	PSMA3,PSMB1,PSMD11,PSMD8,PSME2,PSME3
Metabolic pathways	28	0,0129	ACO-T8,AK1,ALDOC,ALOX12,AMY1A,ANPEP,ATP5B,ATP5F1,BLVRA,CBR1,CNDP2,ECHS1,FAH,GNPDA1,GPT,HSD17B4,LTA4H,MAN1A1,MDH1,NT5C,PGD,PNP,PRPS2,PTGS1,PYGL,RPN2,TALDO1,UQCRC1
Pentose phosphate pathway	4	0,0202	ALDOC,PGD,PRPS2,TALDO1
Arachidonic acid metabolism	5	0,0202	ALOX12,CBR1,GPX3,LTA4H,PTGS1
Carbon metabolism	7	0,0202	ALDOC,ECHS1,GPT,MDH1,PGD,PRPS2,TALDO1
Endocytosis	10	0,0202	AR-F3,ARPC4,DAB2,DNM2,FAM21A,HSPA8,IST1,RAB5B,SH3KBP1,VPS35
Tight junction	8	0,0202	ACTN4,CLDN5,JAM3,LLGL2,MYH14,MYH8,MYL6,TUBA8
Phospholipase D signaling pathway	7	0,0269	DNM2,FCER1G,GNAS,GRB2,GRM7,NRAS,RRAS
Thyroid hormone synthesis	5	0,0299	ALB,GNAS,GPX3,SERPINA7,TG
Aminoacyl-tRNA biosynthesis	4	0,0317	DARS,GARS,HARS,MARS
Regulation of actin cytoskeleton	8	0,0323	AC-TN4,ARPC4,IQGAP2,MYH14,NRAS,PPP1CA,PPP1R12B,RRAS
Glutathione metabolism	4	0,039	ANPEP,GPX3,GSTP1,PGD
Platelet activation	6	0,039	COL1A1,FCER1G,GNAS,PPP1CA,PTGS1,STIM1

B

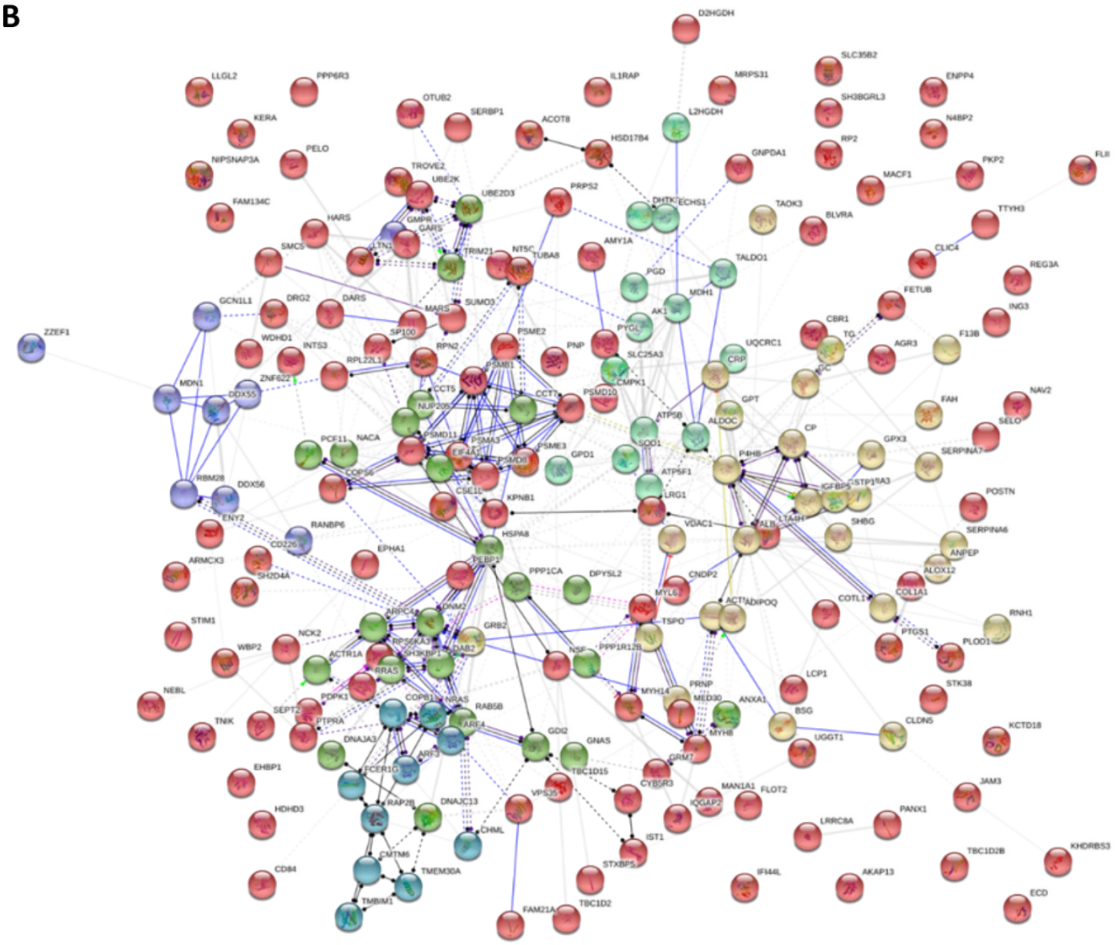

Figure S7. Enrichment in KEGG pathways (A) and networks (B) based on STRING annotation tool applied on the list of the exclusively L-CNC proteins. Network edges are based on molecular action (Kmeans clustering n=6). FDR= False Discovery Rate.

Characterization of CNC film coated coverslips.

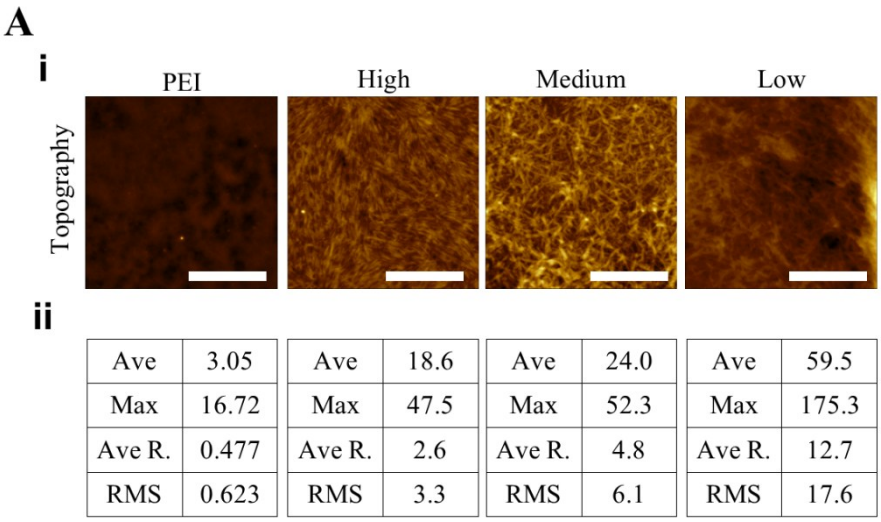

Ave	3.05	Ave	18.6	Ave	24.0	Ave	59.5
Max	16.72	Max	47.5	Max	52.3	Max	175.3
Ave R.	0.477	Ave R.	2.6	Ave R.	4.8	Ave R.	12.7
RMS	0.623	RMS	3.3	RMS	6.1	RMS	17.6

Figure S8. (A) AFM topographies of PEI and 1 wt.% CNC films (i) and roughness parameters (ii): average height (AVE); maximum height (Max); average roughness (Ra); root mean square roughness (RMS). Scale bar: 1 μm.

hASCs behavior on CNC coated coverslips after PL incubation. At day 2, cells seeded on CNC film coatings pre-incubated with PL showed similar proliferation rate in all groups (Fig. S7B). On the other hand, whereas H-CNC group did not exhibit significant cell proliferation from day 2 to day 7, cells seeded onto L-CNC and, in particular, M-CNC significantly increased proliferation. By day 28, all conditions increased the number of cells, but no significant differences could be observed among tested conditions. Interestingly, although hASCs morphology during the first few days (day 2) was also very similar, considerable differences between groups start to be noticed by day 7 (Fig. S7A).

Whereas hASCs cultured on H-CNC showed a highly elongated morphology, on M-CNC films they exhibited a spindle-like shape and on L-CNC formulation they tended to form dense cell clusters. These morphological characteristics were maintained over the time in culture up to day 28 (Fig. 3A and S7).

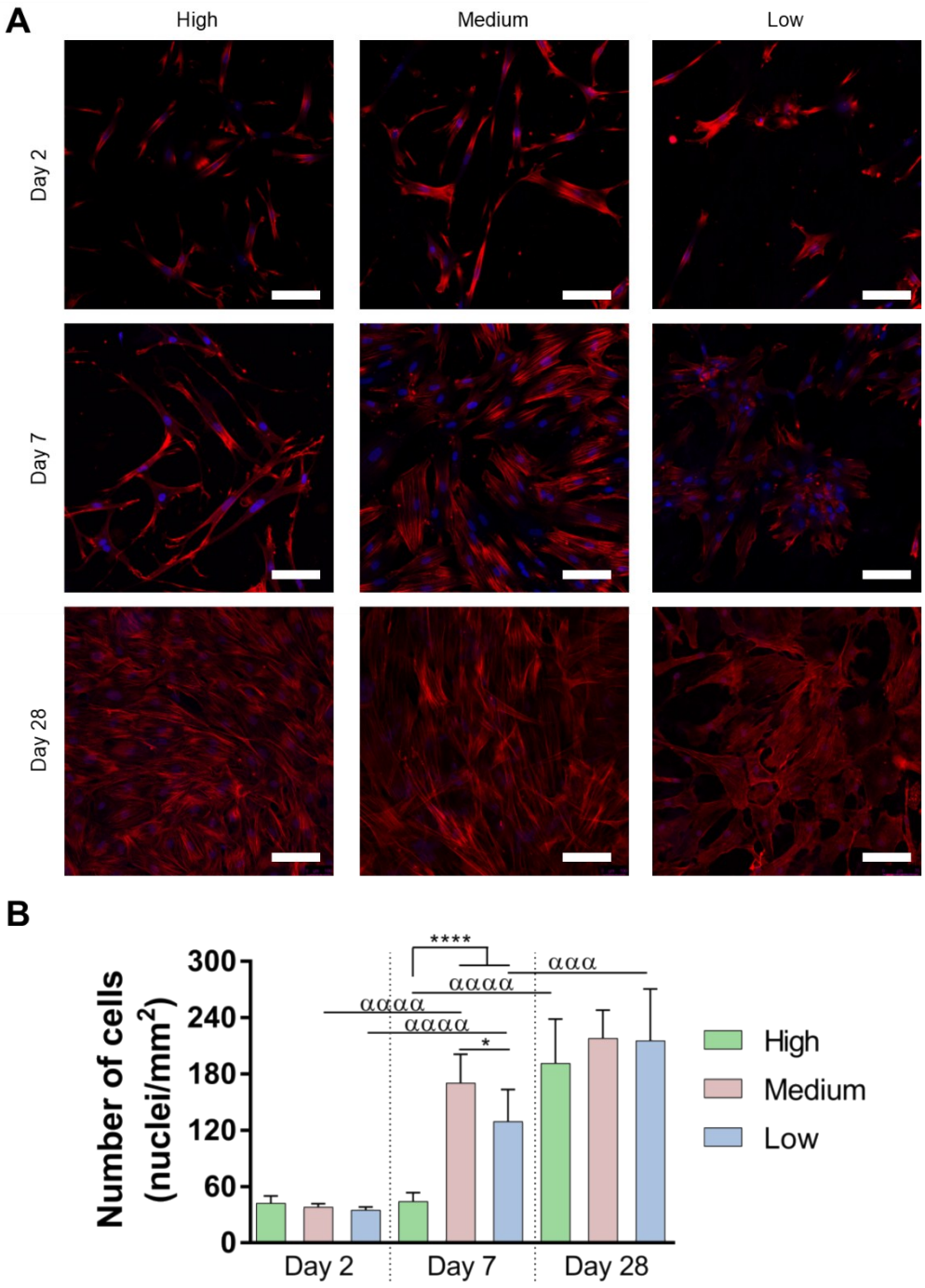

Figure S9. *In vitro* evaluation of hASCs behaviour. (A) Fluorescence microscopy images showing cell morphology after 2, 7 and 28 days in culture. Staining actin (red) and nuclei

(blue). (B) Analysis of cell proliferation rate. Statistical significance: '*'- between formulations and 'α' - between timepoints. Scale bar: 100 µm.

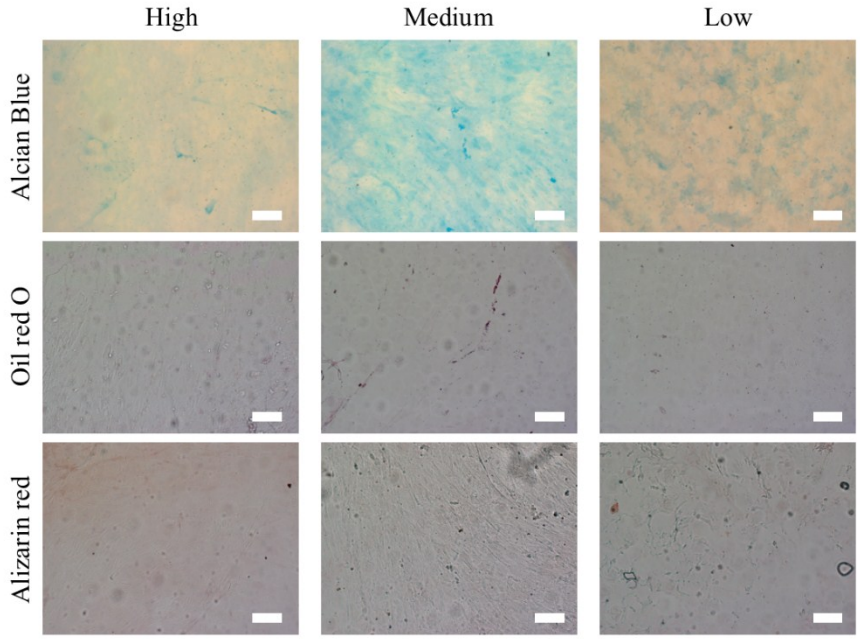

Figure S10. Analysis of hASCs commitment to the chondrogenic (Alcian Blue staining), adipogenic (Oil red O staining) and osteogenic (Alizarin red staining) lineages. Potential chondrogenesis can be indicated by the increase of sulfated GAGs content that stain with Alcian Blue (top); adipogenesis would be indicated by the accumulation of neutral lipid vacuoles that stain with Oil red O (middle); and osteogenesis would be indicated by the increase of calcium deposition (bottom). None of the different formulations analyzed stained for oil red O and Alizarin red stainings. Scale: 50 µm.

References

[1] Saúde D-G d 2012 Norma 010/2012: Utilização Clínica de Concentrados Plaquetários no Adulto. In: *Norma da Direcção-Geral da Saúde* (Portugal

[2] Schwartz J, Padmanabhan A, Aqui N, Balogun R A, Connelly-Smith L, Delaney M, Dunbar N M, Witt V, Wu Y and Shaz B H 2016 Guidelines on the Use of Therapeutic Apheresis in Clinical Practice–Evidence-Based Approach from the Writing Committee of the American Society for Apheresis: The Seventh Special Issue *J. Clin. Apheresis* **31** 149-338

[3] Slichter S J 2007 Evidence-Based Platelet Transfusion Guidelines *Hematology Am. Soc. Hematol. Educ. Program* 172-8

[4] Mendes B B, Gómez-Florit M, Babo P S, Domingues R M, Reis R L and Gomes M E 2018 Blood derivatives awaken in regenerative medicine strategies to modulate wound healing *Advanced Drug Delivery Reviews* **129** 376-93

[5] Bondeson D, Mathew A and Oksman K 2006 Optimization of the isolation of nanocrystals from microcrystalline celluloseby acid hydrolysis *Cellulose* **13** 171

[6] Domingues R M A, Silva M, Gershovich P, Betta S, Babo P, Caridade S G, Mano J F, Motta A, Reis R L and Gomes M E 2015 Development of Injectable Hyaluronic Acid/Cellulose

Nanocrystals Bionanocomposite Hydrogels for Tissue Engineering Applications *Bioconjugate Chemistry* **26** 1571-81

[7] Beck S, Méthot M and Bouchard J 2015 General procedure for determining cellulose nanocrystal sulfate half-ester content by conductometric titration *Cellulose* **22** 101-16

[8] Schindelin J, Arganda-Carreras I, Frise E, Kaynig V, Longair M, Pietzsch T, Preibisch S, Rueden C, Saalfeld S, Schmid B, Tinevez J-Y, White D J, Hartenstein V, Eliceiri K, Tomancak P and Cardona A 2012 Fiji: an open-source platform for biological-image analysis *Nature Methods* **9** 676-82

[9] Kozlowski L P 2016 IPC – Isoelectric Point Calculator *Biology Direct* **11** 55

[10] Carvalho P P, Wu X, Yu G, Dias I R, Gomes M E, Reis R L and Gimble J M 2011 The effect of storage time on adipose-derived stem cell recovery from human lipoaspirates *Cells, tissues, organs* **194** 494-500